ANALYSIS AND CONTROL OF TORQUE PULSATIONS IN CURRENT FED INDUCTION MOTOR DRIVES

T. A. LIPO

General Electric Company
Schenectady, New York

SUMMARY

Three types of feedback compensation schemes are described which can be used to reduce the torque pulsations which normally occur when induction machines are supplied from a current source inverter. The approach is verified both by a detailed computer simulation and also by test results from an actual system. Limitations of the method near zero slip frequency (no load) is discussed and a means suggested for elimination of the problem.

INTRODUCTION

Most inverters in present use can be designated as adjustable frequency voltage sources since the output terminal voltage is essentially independent of current. Recently, however, the useful features of current source inverters have been recognized in which the current rather than the voltage appears as the independent variable. The current source inverter drive is particularly appealing for use in four quadrant single motor drives. However, a serious drawback to the use of a current source inverter in such applications is the harmonic torque pulsations which exist at multiples of six times the output frequency of the inverter. In these applications shaft mechanical resonances often occur, generally in the range 30-100 Hz. These resonances are usually not of concern over most of the speed range. However, during starting or reversing operations the stator line frequency becomes sufficiently low that the sixth harmonic component of pulsating torque lies in the range of mechanical resonance. Operation continuously at such a resonance condition could result in abnormal wearing of gear teeth or shaft fatigue. In some cases, for example in machine tool drives, the presence of these torque pulsations are sufficiently large to affect the performance of the system even when not operating near a mechanical resonance.

When voltage source inverters are used in such applications, pulse-width-modulation is employed whereby the basic six step waveshape is modulated so as to eliminate the harmonic voltage components responsible for the sixth harmonic torque pulsation [1]. Unfortunately, application of pulse-width-modulation to current source inverters is more difficult [2]. Since the current source inverter employs 120 degree commutation only two of the three phases of the motor can be modulated at any instant. This results in a modulation scheme which is less desirable than that used in a voltage inverter which employs 180 degree commutation. Also the modulation algorithm is much more complex than the simple sine-triangle wave modulation typically used with voltage inverters. Losses in the machine are increased substantially and,

Electric Machines and Electromechanics: An International Quarterly, 3:357-368

0361-6967/79/020357-12$2.25

although the lowest frequency torque pulsation can be eliminated higher harmonics are increased to the point where they too can create resonance problems.

Although attempts have been made to program the DC link current in an open loop fashion, such an approach is difficult over a range of load and speed and is subject to the usual deterioration in performance due to parameter changes [3]. This paper describes a different approach to the elimination of torque pulsations in current source induction motor drives by feedback control of the DC link current. Three different types of implementations increasing in complexity are described and the advantages and disadvantages of each are described. Practical application aspects of the control is discussed. The approach is verified both by a detailed computer simulation and on an actual system.

BASIC OPERATION

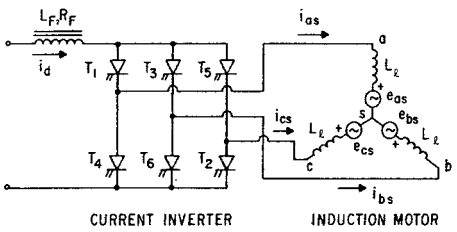

Fig. 1 Simplified Current Source Inverter Drive

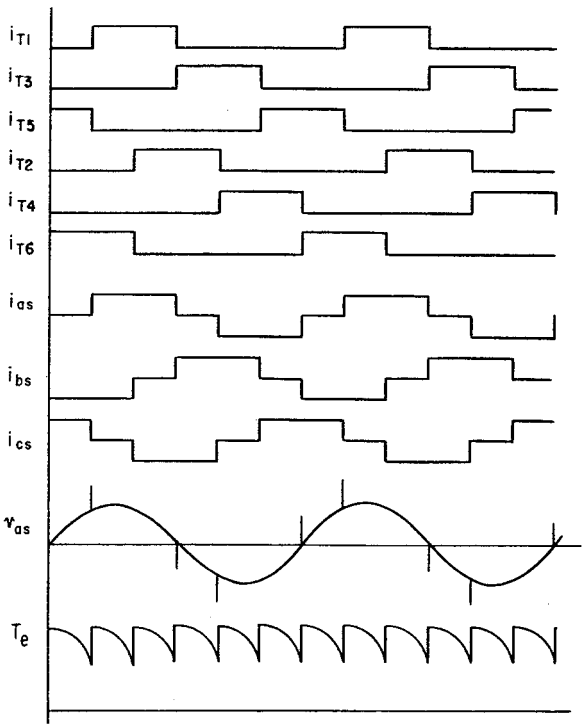

Fig. 2 Idealized Current, Voltage and Torque Waveforms.

The basic three phase bridge configuration of a current source inverter drive is illustrated in Fig. 1, which omits the auxiliary circuitry that is required to force-commutate the thyristors. The inverter is fed with a controlled current i_d which, ideally, has negligible ripple and is sequentially switched from phase to phase of the motor load. Only two thyristors conduct at any given time, each carrying the impressed direct current for 120 degrees of the fundamental output period, except for commutation overlap. The resulting motor line currents have a waveform similar to the AC line current produced by a conventional six pulse voltage-fed rectifier as shown in Fig. 2.

During steady-state operation, an induction motor can be represented as an equivalent counter-emf in series with a small impedance. It can be noted that even though the currents are square wave in nature, the motor terminal voltage is essentially sinusoidal with voltage transients (spikes) superimposed at the instants of commutation. These transients appear across the motor leakage reactance and are generated by the commutating circuit. To produce instantaneous current transfer, as indicated by the ideal waveforms of Fig. 2, infinite impulse

voltages would be necessary. In practice, however, the finite commutating voltage requires a non-zero time interval to force the current change through the leakage inductance.

The presence of a sinusoidal counter-emf implies that the air gap flux linkages are also nearly sinusoidal. Interaction of the sinusoidal air gap flux with the piece-wise constant stator currents result in a torque pulsation which resembles the output voltage of a conventional six pulse controlled rectifier bridge. This torque pulsation has a fundamental frequency equal to six times the inverter output frequency [4].

DESCRIPTION OF FEEDBACK APPROACH

A block diagram representation of a typical current source induction motor drive system is shown in Fig.3. In general the system is equipped with a feedback control system which is employed to satisfy the system performance requirements. This control is represented simply as a box in Fig. 3. The control may have a variety of inputs depending upon the control scheme but typically employs stator current, air gap flux and rotor speed [5]. Many other feedback schemes are possible. However, regardless of the feedback variables only two system inputs are available for control, namely the frequency of the current source inverter and the phase delay angle of the rectifier bridge. In most cases a fast inner current loop is incorporated in the rectifier control system so that, effectively, the DC link current can be considered as the second system input. The commanded values of the inverter angular frequency and rectifier output current determined by the control system are ω_e^* and α^* respectively. The inverter frequency is, in essence, the cause of the torque pulsation and use of this input to reduce torque pulsation would involve a type of pulse-width-modulation scheme mentioned previously. It is evident that the other control input might also provide a means for reducing torque pulsations if the DC link current can be "modulated" in the proper manner. The required modulation can be determined inherently if the undesirable quantity (torque pulsation) is detected and regulated to a minimum by means of feedback as illustrated in Fig. 3. Note that only the pulsating component of torque need be fed back to the summing junction since the average value is essentially fixed by the main control block.

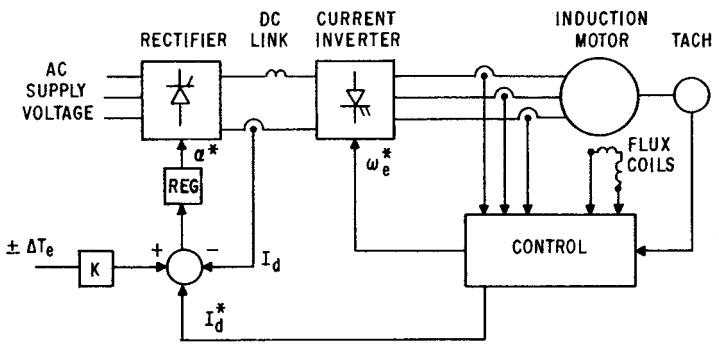

Fig. 3 Typical Control System Showing Added Input for Decogging Signal.

Method 1 - Using Motor Line Current and Rotor Speed

Because of the coupling which exists between phases of a three phase symmetrical induction machine it has been found useful to employ a transformation of variables resulting in an equivalent two phase machine [6]. In

general, these equations are dependent upon the speed of the frame used to view the machine. However, when the reference frame is stationary or "fixed to the stator" the machine equations can be written [6]

$$v_{qs} = r_s i_{qs} + d\lambda_{qs}/dt \tag{1}$$

$$v_{ds} = r_s i_{ds} + d\lambda_{ds}/dt \tag{2}$$

$$0 = r_r i_{qr} + d\lambda_{qr}/dt - \omega_r \lambda_{dr} \tag{3}$$

$$0 = r_r i_{dr} + d\lambda_{dr}/dt + \omega_r \lambda_{qr} \tag{4}$$

$$T_e = \frac{3P}{4} (\lambda_{ds} i_{qs} - \lambda_{qs} i_{ds}) \tag{5}$$

The number of equations involved even with equivalent two phase variables is large and it is convenient to view the machine variables as components of vector quantities [7]. Let

$$\hat{v}_s = v_{qs}\hat{u}_q + v_{ds}\hat{u}_d \tag{6}$$

$$\hat{i}_s = i_{qs}\hat{u}_q + i_{ds}\hat{u}_d \tag{7}$$

$$\hat{\lambda}_s = \lambda_{qs}\hat{u}_q + \lambda_{ds}\hat{u}_d \tag{8}$$

$$\hat{\omega}_r = \omega_r \hat{u}_n \tag{9}$$

where $\hat{u}_d$ and $\hat{u}_q$ denote unit vectors in the two phase d- and q-axes respectively. Similar definitions apply for the rotor variables. Equations 1-5 can be written in vector form as

$$\hat{v}_s = r_s \hat{i}_s + d\hat{\lambda}_s/dt \tag{10}$$

$$\hat{0} = r_r \hat{i}_r + d\hat{\lambda}_r/dt - \hat{\omega}_r \times \hat{\lambda}_r \tag{11}$$

$$\hat{T}_e = \frac{3P}{4} \hat{\lambda}_s \times \hat{i}_s \tag{12}$$

By means of auxiliary equations relating the flux linkages and currents [6] it is possible to solve for $\hat{i}_r$ and $\hat{\lambda}_s$ in terms of $\hat{i}_s$ and $\hat{\lambda}_r$ as

$$\hat{\lambda}_s = (L_{\ell s} + k_r L_{\ell r})\hat{i}_s + k_r \hat{\lambda}_r \tag{13}$$

$$\hat{i}_r = \hat{\lambda}_r/(L_{\ell r} + L_m) - k_r \hat{i}_s \tag{14}$$

where

$$k_r = L_m/(L_m + L_{\ell r}) \tag{15}$$

When written only in terms of stator current and rotor flux linkage the equations which define transient behavior of the machine, Eqs. 10-12, can now be expressed as

$$\hat{v}_s = r_s \hat{i}_s + (L_{\ell s} + k_r L_{\ell r}) \hat{i}_s + k_r d\hat{\lambda}_r/dt \tag{16}$$

$$k_r r_r \hat{i}_s = r_r \hat{\lambda}_r/(L_m + L_{\ell r}) + d\hat{\lambda}_r/dt - \hat{\omega}_r x \hat{\lambda}_r \tag{17}$$

$$\hat{T}_e = \frac{3P}{4} k_r \hat{\lambda}_r x \hat{i}_s \tag{18}$$

Note that Eq. 17 has been written so that the stator current appears on the left hand side. This form of the equation suggests that if the actual motor line currents which flow in the physical system can be measured then signals proportional to the two phase stator currents can be constructed and applied to an on-line model of the rotor circuits of the machine. The cross product of the measured stator current and calculated rotor flux linkage can be used to compute the electromagnetic torque. The pulsating value of torque can be obtained by eliminating the average component by means of a high pass filter. The resulting signal, ΔT_e, corresponds to the pulsating (zero average) component of T_e.

Figure 4 shows a practical implementation of this control scheme. It can be noted that since actual stator current is used as inputs to the model, changes in stator resistance and stator leakage inductance due to temperature, frequency (skin effect) and tooth saturation do not affect its accuracy. However, measured values of magnetizing inductance, rotor leakage inductance and rotor resistance are used as constant coefficients in the model. Hence, changes in the corresponding actual machine parameters will affect the accuracy of the torque computation. Probably the most significant parameter change occurs in rotor resistance as the motor heats up during use. If necessary, this effect can be compensated by changing the modeled value of rotor resistance as a function of frame temperature. The order of improvement resulting from this simple compensation scheme is probably sufficient for most routine applications. If necessary, more accurate compensation could be introduced by an on-line model of the thermal system.

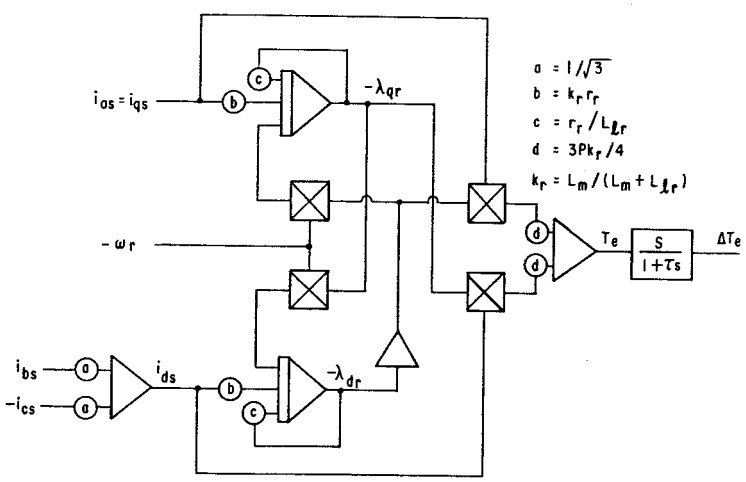

Figure 4 Implementation of Method 1.

Method 2 - Using Terminal Voltage and DC Link Current

Although electromagnetic torque is most often calculated as the cross product of stator flux and stator current as in Eq. 12, many other equivalent forms for the torque equation exist. In particular, if stator flux linkage is expressed in terms of a leakage component plus an air gap component then

$$\hat{\lambda}_s = L_{\ell s}\hat{i}_s + \hat{\lambda}_m \tag{19}$$

In terms of air gap flux linkage

$$\hat{T}_e = \frac{3P}{4}\hat{\lambda}_m x \hat{i}_s \tag{20}$$

since the cross product of any vector with itself is identically zero. It can be recalled from vector algebra that the cross product can be expressed equivalently as

$$T_e = \frac{3P}{4}\left[|\hat{i}_s|\,|\hat{\lambda}_m|\sin\theta\right] \tag{21}$$

where the vertical bars imply the magnitude of the vector and θ is the instantaneous angle between vectors.

The quantity inside the brackets, namely $|\lambda_m|\sin\theta$, can be interpreted as the instantaneous component of the flux linkage vector normal to the current vector. This interpretation of the cross product suggests a means for computing the instantaneous pulsating torque from terminal measurements. Consider, for example, the time instant when the DC link current is directed into the c phase terminal and out of the b phase terminal with the a phase circuit open circuited or "floating" as shown in Fig. 5. From the definition of the d-q two phase variables it can be shown that the two components of the vector $\hat{\lambda}_m$ are

$$\lambda_{qm} = \lambda_{am} = \int v_{am}\,dt \tag{22}$$

$$\lambda_{dm} = (\lambda_{cm} - \lambda_{bm})/\sqrt{3}$$

$$= (1/\sqrt{3})\int (v_{cm} - v_{bm})\,dt \tag{23}$$

From Eq. 21 note that the torque producing component of flux linkage is, at this instant, the q-axis component since this component is normal to the current vector during the 60 degree portion of a cycle wherein this connection applies. The q-axis component is simply equal to the a phase component of flux linkage since the q-axis and a-phase axis are magnetically aligned by definition [6]. Since the a-phase current is zero over this interval it is clear that the voltage measured at the terminals of phase a is identically equal to the air gap voltage and the integral of this voltage if the flux linkages associated with phase a. If desired this signal can be obtained using only line-to-line voltages so that the neutral need not be available [6]. Although one specific inverter connection was used as an example, these conclusions are general and can be applied to any of the six possible inverter connections. It is clear that the integration must always begin at each commutation so that the initial condition of the integral cannot be found without added information. Only the change in flux linkage over the inverval can be calculated. This component, however, is identically equal to the component which is responsible for the torque pulsation. Again, the unwanted average component of flux linkage can be removed with a high pass filter.

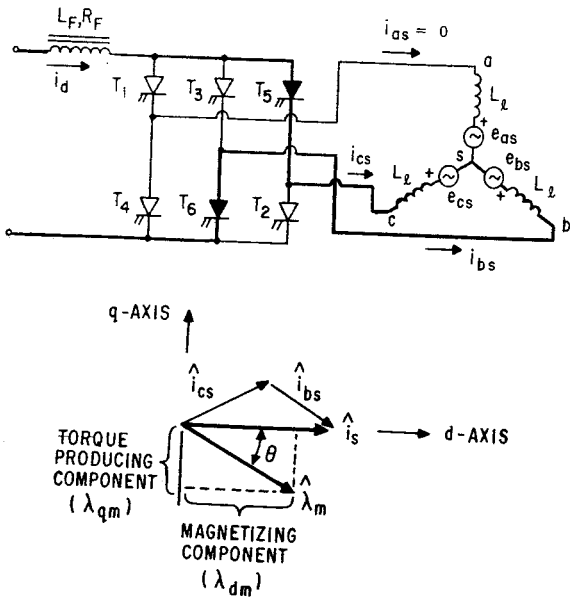

Fig. 5 Circuit Connection Diagram with Thyristors T5 and T6 Conducting.

A mechanization of a torque pulsation measurement scheme employing this approach is shown in Fig. 6. The array of three switches are used to always connect the open circuited phase to the integrator. The other pair of switches is used to select the proper polarity of the open phase. The integrator is reset to zero at the start of each commutation by a series of pulses at frequency rate $6f_e$ or six times the inverter frequency. Since the average DC component of the integrator is not of concern this unwanted component is removed with a high pass filter. The product of the remaining, pulsating component of the integrator output times the DC link current is proportional to the pulsating torque.

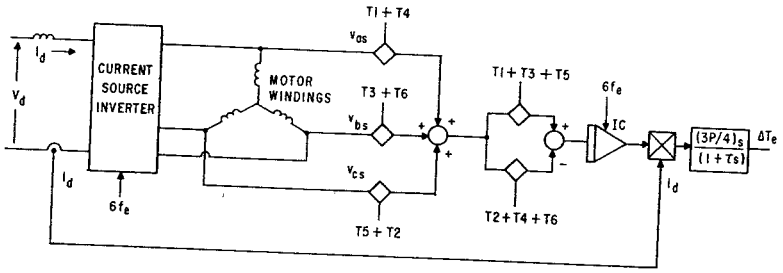

Fig. 6 Implementation of Method 2.

Because the torque producing component of flux linkage and current are measured exactly in Method 2, accuracy is not affected by parameter changes due to saturation, temperature or other effects. However, the method assumes that commutation of the current source inverter is accomplished in negligible time compared to the basic 60 degree conduction interval. This assumption becomes less and less valid as the frequency increases. Nevertheless, a useful signal can be derived below 20 Hz line frequency (120 Hz torque pulsation) which is the region of primary concern.

Method 3 - Using Air Gap Voltage and Motor Line Current

The two previous methods which involve only terminal measurements are generally sufficiently accurate for most applications. However, when stringent restrictions are placed on torque pulsations it may be necessary to resort to internal measurements of the state of the machine. Figure 7 shows a scheme which employs search coils which are inserted in the top of the stator slots and are designed to measure the voltage corresponding to the air gap component of flux. The coils are designed to couple only with the useful, fundamental component of air gap flux. Other, unwanted components arise from saturation and rotor slot harmonics which do not produce useful torque. These components can be eliminated from the air gap voltage measurement by proper interconnection and weighting of the coil voltages [8]. Integration of the search coil voltages produces signals proportional to air gap flux linkages. The two phase stator currents can again be found algebraically from the three phase currents. Cross product multiplication of the two phase air gap flux linkage and stator current signals by means of Eq. 20 yields the motor torque. Again, if desired, the unneeded average value can be removed by a high pass filter.

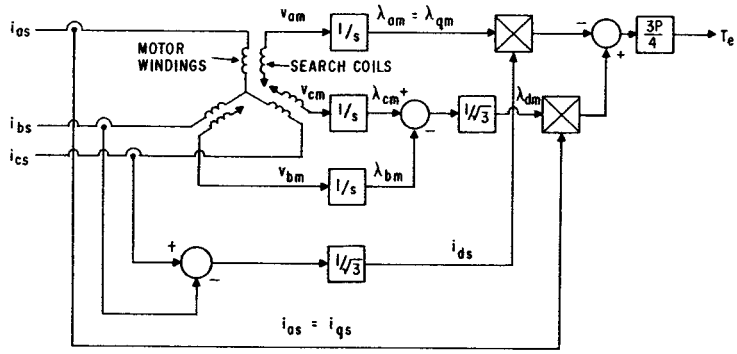

Fig. 7 Implementation of Method 3.

COMPUTED AND MEASURED RESULTS

Three methods for computing pulsating torque have been described which can be used as a "decogging" signal for modulating the DC link current as shown in Fig. 3. In order to verify the effectiveness of the approach the three feedback strategies were studied on a hybrid computer incorporating a detailed representation of motor and inverter [6,9]. For convenience the rectifier was modeled as an ideal power amplifier so that the desired output DC voltage was instantly obtained without sampling delay. The induction machine used for purposes of this study was a 230 V, 4 pole, 25 hp induction machine having the following parameters: $r_s = 0.0788\,\Omega$, $r_r = 0.0408\,\Omega$, $x_{\ell s} = 0.2122\,\Omega$, $x_{\ell r} = 0.4362\,\Omega$, $x_m = 5.54\,\Omega$. Base frequency used to compute the above reactances was 60 Hz. The DC link inductance was 29.2 mH.

Figure 8 shows a computer trace of a typical operating condition when the feedback decogging signal is out of service. The operating condition corresponds to a line frequency of 3.6 Hz, slip frequency of 1.2 Hz and link current of 60 A resulting in an average electromagnetic torque of 55 Nm or approximately one-half rated value. The large pulsating component superimposed on the average value of torque is apparent. In Fig 9 the feedback decogging signal has been installed using control method 3. A large reduction in the pulsating torque is clearly evident. Similar results were also observed for the other two control methods since the identity of the feedback signal is essentially the same.

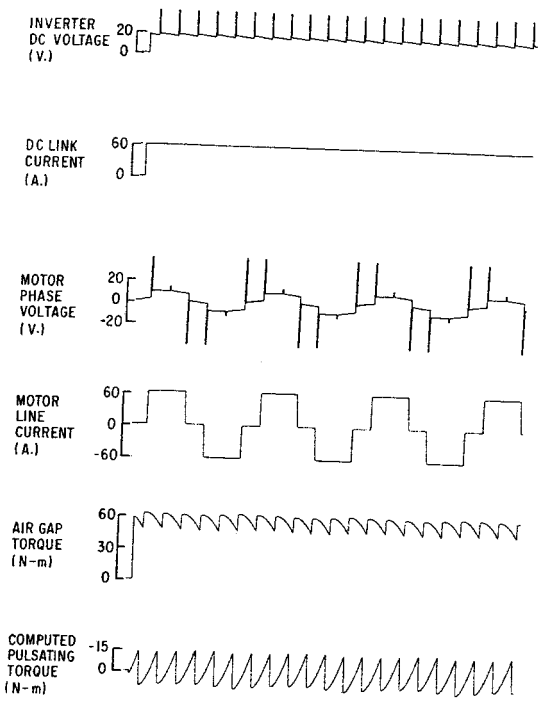

Fig. 8. Simulation Result with Decogging Signal Out of Service. Stator Frequency 3.6 Hz, Slip Frequency, 1.2 Hz, DC Link Current 60 A.

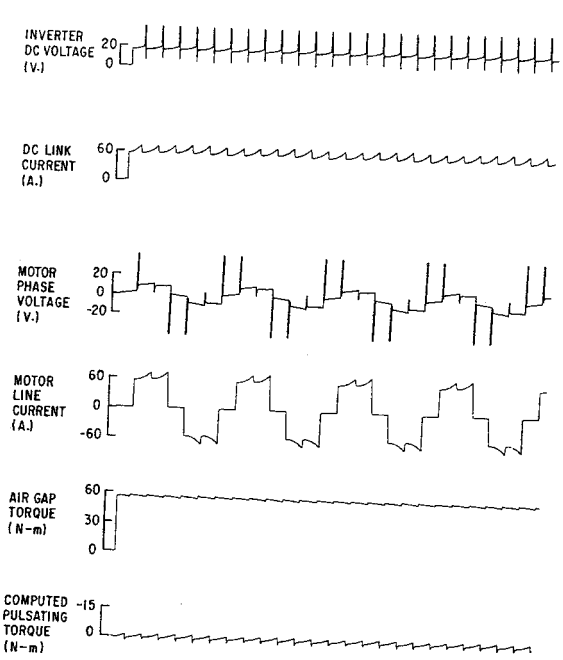

Fig. 9 Simulation Result with Decogging Signal in Service. Operating Conditions Same as Fig. 8.

Figures 10 and 11 show scope traces taken from an actual experimental system. In Fig. 10 the decogging signal is out of service. It can be noted that the measured torque very closely resembles the torque pulsations predicted by the computer simulation. The basic sixth harmonic pulsation in the torque can be observed. As a practical matter much higher frequency components in the line current and torque can be observed which are not apparent in the simulation traces. These components arise from the 360 Hz ripple in DC link current resulting from harmonics contributed by the phase controlled rectifier. In Fig. 11 the feedback decogging has been installed using Method 3. It is evident that a substantial reduction in pulsating torque can be achieved in practice as well as in theory. Fourier Analysis of the torque traces in Figs. 10 and 11 indicate that a ten to one reduction in pulsating torque can be readily obtained.

PRACTICAL CONSIDERATIONS

Although the feedback scheme which has been described functions equally well in the regenerative mode as in motoring, it is interesting that the polarity of the proper feedback signal changes sign. The needed sign change can be easily incorporated into the control but the proper feedback polarity becomes ambiguous at no load. Instability will result for either polarity at

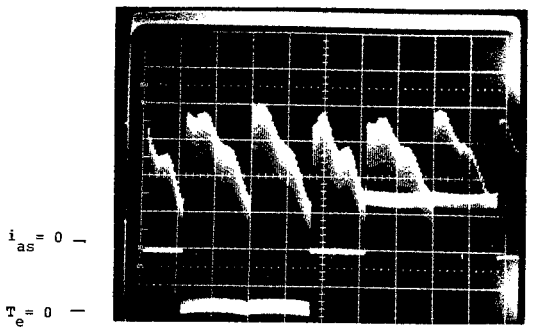

Fig. 10 Experimental Results from Actual Drive System with Decogging Signal Out of Service. Top Trace: Electromagnetic Torque, Scale 31 Nm Nm/div. Bottom Trace: Motor Line Current, Scale 75 A/div., Time Scale 50 ms/div.

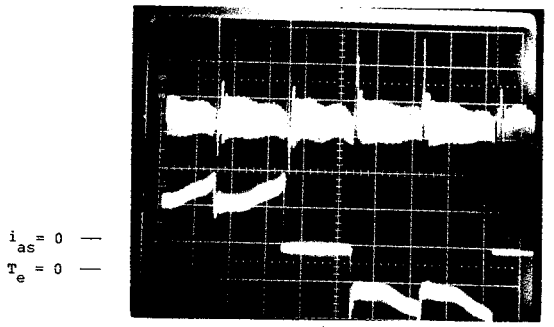

Fig. 11 Experimental Results with Decogging Signal in Operation. Scales same as Fig. 10.

no load if the system gain is too high. A reduction in feedback gain can be avoided and torque pulsation kept at a low value if the air gap flux is reduced near the no load condition by use of the main system control. This strategy is often desirable for other purposes since the no load losses consisting mainly of iron losses will be reduced substantially at the same time. Figure 12 shows a series of computer traces illustrating a transition from motoring to regeneration by reducing the air gap flux. The pulsating torque clearly remains small during the entire transition.

Another practical matter involving implementation of such a control is speed of response. Certainly, when substantial changes in torque are required by the main system control it must not be interpreted as "pulsating torque" and eliminated by the decogging system. Since pulsating torque considerations are secondary when it is desired to move rapidly from one operating condition to another, one solution is to switch this signal out when the torque change exceeds some threshold. Alternatively, changes in operating condition can be sensed directly from the command signal i_d^*. Figure 13 describes a "riding gain" type of decogging control signal in which the feedback gain is inversely proportional to the change in command signal i_d^*.

CONCLUSION

This paper has presented three methods for feedback control of the pulsating torque which occurs when an induction motor is supplied from a current source inverter. Practical problems involved in the implementation of each have been discussed and it is demonstrated that a significant reduction in pulsating torque can be achieved in a practical system. Although this paper has concerned itself with induction motor drives it is clear the similar improvements can be attained by modulating the DC link of load commuted synchronous motor drives.

ACKNOWLEDGEMENT

The assistance of J.D. D'Atre and A.B. Plunkett during the experimental phase of this investigation is gratefully acknowledged.

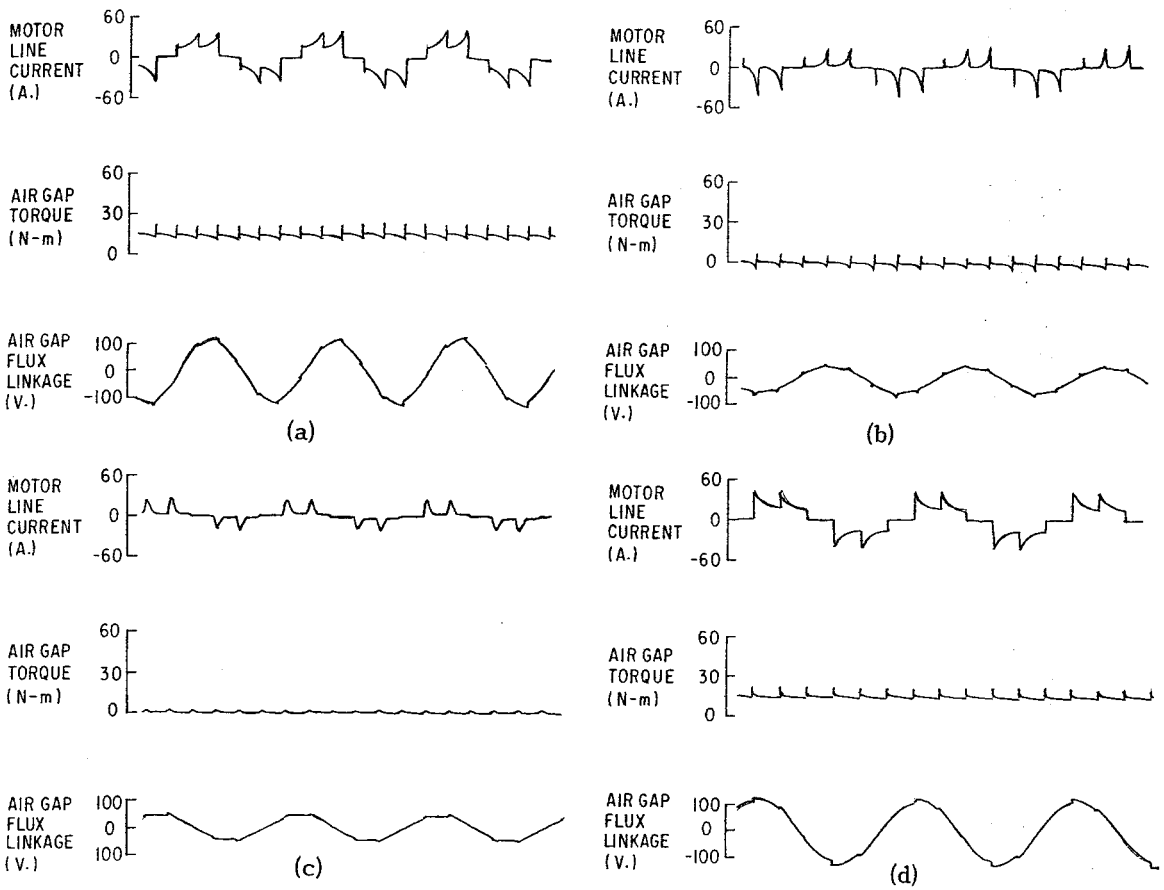

Fig. 12 Simulations Traces Showing Operation Through No-Load Using Weakened Air Gap Flux. a) Rated Flux, OneEighth Rated Motor Load, b) Reduced Flux, No-Load, Positive Polarity Feedback, c) Reduced Flux, No-Load, Negative Polarity Feedback, d) Rated Flux, One-Eighth Regenerative Load.

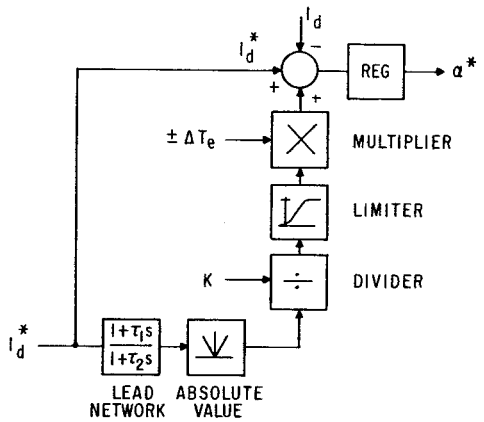

Fig. 13 Decogging Control System Employing Riding Gain.

REFERENCES

1. A. Schonung and H. Stemmler, "Static frequency changers with 'Sub-harmonic' control in conjunction with reversible variable speed AC drives", Brown Boveri Review, August/September 1964, pp. 555-577.
2. M. Blumenthal, "Pulse angle modulated operation of an ac machine fed by a current source inverter", Conference Record of the International Conference on Electrical Machines, 13-15 September, 1976, pp. I1-11 to I1-18.
3. T.H. Chin, "A new controlled current type inverter with improved performance", IEEE/IAS International Semiconductor Power Converter Conf. Record, 28-31 March 1977, pp. 185-192.
4. T.A. Lipo and E.P. Cornell, "State-variable steady-state analysis of a controlled current induction motor drive". IEEE Trans. on Industry Applications, vol. IA-11, No. 6, November/December 1975, pp. 704-712.
5. A.B. Plunkett, J.D. D'Atre and T.A. Lipo, "Synchronous control of a static AC induction motor drive", Conference Record of the 1977 IEEE/IAS Annual Meeting, Oct. 26, 1977, pp. 609-615.
6. P.C. Krause and C.H. Thomas, "Simulation of symmetrical induction machinery", IEEE Trans. on Power Apparatus and Systems, vol. PAS-84, Nov. 1965, pp. 1038-1053.
7. K.P. Kovacs and I. Racz, "Transient behavior of AC machines", (book) Hungarian Academy of Science, Budapest, 1959 (In German).
8. T.A. Lipo, "Flux sensing and control of static AC drives by the use of flux coils", IEEE Trans. on Magnetics, vol. MAG-13, No. 5, September 1977, pp. 1403-1408.
9. T.A. Lipo, "Simulation of a current source inverter drive", Power Electronics Specialists Conference Record, June 14-16, 1977, pp. 310-315.

Appendix

Analog Computer Symbols

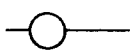
Potentiometer

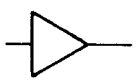
Inverter/Summer (sign inverting)

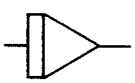
Integrator (sign inverting)

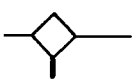
Logic Controlled SPST Analog Switch


Multiplier

Manuscript received in the final form, January 22, 1979